

COMMUNICATION

Depressed neuromuscular transmission causes weakness in mice lacking BK potassium channels

 Xueyong Wang¹, Steven R.A. Burke² , Robert J. Talmadge³, Andrew A. Voss² , and Mark M. Rich¹ 

Mice lacking functional large-conductance voltage- and Ca^{2+} -activated K^+ channels (BK channels) are viable but have motor deficits including ataxia and weakness. The cause of weakness is unknown. In this study, we discovered, *in vivo*, that skeletal muscle in mice lacking BK channels ($\text{BK}^{-/-}$) was weak in response to nerve stimulation but not to direct muscle stimulation, suggesting a failure of neuromuscular transmission. Voltage-clamp studies of the $\text{BK}^{-/-}$ neuromuscular junction (NMJ) revealed a reduction in evoked endplate current amplitude and the frequency of spontaneous vesicle release compared with WT littermates. Responses to 50-Hz stimulation indicated a reduced probability of vesicle release in $\text{BK}^{-/-}$ mice, suggestive of lower presynaptic Ca^{2+} entry. Pharmacological block of BK channels in WT NMJs did not affect NMJ function, surprisingly suggesting that the reduced vesicle release in $\text{BK}^{-/-}$ NMJs was not due to loss of BK channel-mediated K^+ current. Possible explanations for our data include an effect of BK channels on development of the NMJ, a role for BK channels in regulating presynaptic Ca^{2+} current or the effectiveness of Ca^{2+} in triggering release. Consistent with reduced Ca^{2+} entry or effectiveness of Ca^{2+} in triggering release, use of 3,4-diaminopyridine to widen action potentials normalized evoked release in $\text{BK}^{-/-}$ mice to WT levels. Intraperitoneal application of 3,4-diaminopyridine fully restored *in vivo* nerve-stimulated muscle force in $\text{BK}^{-/-}$ mice. Our work demonstrates that mice lacking BK channels have weakness due to a defect in vesicle release at the NMJ.

Introduction

Large-conductance voltage- and Ca^{2+} -activated K^+ channels (BK, Maxi-K, slo1, or KCa1.1 channels) are widely expressed in the nervous system and have been shown to play a central role in the regulation of excitability (Salkoff et al., 2006; Berkefeld et al., 2010; Wang et al., 2014). Mice lacking functional BK channels have impairments that include increased mortality, hearing loss, hypertension, bladder dysfunction, and motor deficits (Meredith et al., 2004; Rüttiger et al., 2004; Sausbier et al., 2005; Halm et al., 2017). The motor deficits include tremor, problems with gait, weak grip, and decreased ability to stay on the rotarod. In humans, mutations in the gene that encodes the BK channel (KCNMA1) are linked with epilepsy, movement disorders, and hypotonia (Bailey et al., 2019). Broadly, motor phenotypes caused by BK channel mutations or loss have been largely attributed to cerebellar dysfunction (Meredith et al., 2004; Sausbier et al., 2004; Chen et al., 2010; Typlt et al., 2013).

Despite evidence suggesting that mice lacking BK channels are weak, we are unaware of studies to determine the mechanism underlying weakness. BK channels are expressed in skeletal muscle (Tricarico et al., 2004; Dinardo et al., 2012) and are

present at the neuromuscular junction (NMJ), where they have been suggested to regulate synaptic function (Robitaille and Charlton, 1992; Robitaille et al., 1993; Vatanpour and Harvey, 1995; Sugiura and Ko, 1997; Pattillo et al., 2001; Flink and Atchison, 2003; Ford and Davis, 2014). The presence of BK channels in muscle and at the NMJ suggests that loss of BK channels in the neuromuscular system could contribute to weakness.

We measured muscle force triggered by stimulation of the sciatic nerve *in vivo* and found a significant reduction of specific force in $\text{BK}^{-/-}$ mice relative to WT. Notably, force generation was normal when the muscle was directly stimulated, suggesting a defect in neuromuscular transmission. Ex vivo voltage-clamp measurements of neuromuscular function revealed a dramatic reduction in the release of synaptic vesicles. Acute pharmacological block of BK channels did not affect NMJ function in WT mice, strongly suggesting that the reduction of vesicle release in $\text{BK}^{-/-}$ mice is independent of BK channel ion current. Block of voltage-gated K^+ channels with 3,4-diaminopyridine (3,4-DAP) to prolong neuronal action potentials normalized NMJ function *ex vivo* and increased force

¹Department of Neuroscience, Cell Biology and Physiology, Wright State University, Dayton, OH; ²Department of Biological Sciences, Wright State University, Dayton, OH; ³Department of Biological Sciences, California State Polytechnic University, Pomona, Pomona, CA.

Correspondence to Mark Rich: mark.rich@wright.edu; Andrew Voss: andrew.voss@wright.edu.

© 2020 Wang et al. This article is distributed under the terms of an Attribution-Noncommercial-Share Alike-No Mirror Sites license for the first six months after the publication date (see <http://www.upress.org/terms/>). After six months it is available under a Creative Commons License (Attribution-Noncommercial-Share Alike 4.0 International license, as described at <https://creativecommons.org/licenses/by-nc-sa/4.0/>).

production *in vivo*. Together, these data suggest that, in the absence of BK channels, Ca^{2+} entry is either reduced or less effective in triggering vesicle release.

Materials and methods

Ethical approval

All procedures involving animals were approved by the Wright State Institutional Animal Care and Use Committee.

Mice

$\text{BK}^{-/-}$ mice were obtained from Andrea Meredith at the University of Maryland (College Park, MD) and a breeding colony established at Wright State University (Dayton, OH). WT littermates were used as controls.

Force measurements

Force measurements were performed as previously reported (Dupont et al., 2019). Mice were anesthetized with isoflurane using a low-flow anesthesia system (SS-01; Kent Scientific), with body temperature maintained at $\sim 35^\circ\text{C}$ using a heat lamp and temperature probe. The plantar flexor muscles (including the lateral and medial gastrocnemius, plantaris, and soleus muscles) and sciatic nerve were exposed by removing the surrounding skin. To minimize the influence of adjacent muscles, the common peroneal and tibial nerves were crushed. During surgery, the muscles were bathed in physiological saline to prevent them from drying out. Mice were then transferred to a custom 3D-printed platform designed to eliminate movement during *in vivo* force recordings. The mouse limb was stabilized with vertical supports and by pinning the limb into recessed areas in the platform that were filled with Sylgard. The platform was mounted to a micromanipulator (XR25/M; Thorlabs). The proximal end of the plantar flexor muscles (Achilles tendon) was attached to the lever of the force transducer (300D-305C dual-mode muscle lever; Aurora Scientific) using 5.0 or 6.0 silk suture and a modified Miller's knot. Optimal length was obtained by measuring the maximum twitch force while lengthening the muscle using the micromanipulator.

Nerve-evoked contractions were stimulated with platinum electrodes resting on the sciatic nerve. Direct muscle contractions were stimulated via platinum electrodes positioned above and below the plantar flexor muscles. For muscle-stimulated contractions, neuromuscular transmission was blocked using $\sim 150 \mu\text{l}$ of 0.5 mg/ml α -bungarotoxin (α -BTX) injected into the gastrocnemius muscles. After injection of α -BTX, neuromuscular block was confirmed by ensuring that the twitch force in response to nerve stimulation was $\le 25\%$ of maximum muscle-stimulated twitch. Stimulus amplitude and the pulse width was $\le 5 \text{ V}$ at 1 ms or $\le 50 \text{ V}$ at 1.5 ms for nerve-stimulated and muscle-stimulated contractions, respectively. A Dagan S-900 Stimulator and S-910 Stimulus Isolation Unit were used for stimulation. Muscle force was recorded and digitized using pClamp10 software (Molecular Devices). For experiments using intraperitoneal injections of 3,4-DAP (Sigma-Aldrich), the drug was diluted with water and injected at a dose of 8 mg/kg animal weight. The average volume injected was 100 μl . 3,4-DAP

was injected immediately after the mice were anesthetized. Force-frequency data were fit with a Boltzmann equation. Data were analyzed with OriginPro 2019 (OriginLab). Data are shown as mean \pm SEM unless otherwise stated.

Voltage-clamp recordings of endplate currents (EPCs)

Mice were sacrificed using CO_2 inhalation, and the tibialis anterior muscle was removed. For most experiments, the recording chamber was continuously perfused with Ringer solution containing (in mM/liter) 118 NaCl , 3.5 KCl , 2 CaCl_2 , 0.7 MgSO_4 , 26.2 NaHCO_3 , 1.7 NaH_2PO_4 , and 5.5 glucose (pH 7.3–7.4, 20–22°C) equilibrated with 95% O_2 and 5% CO_2 . For experiments in low Ca^{2+} /high Mg^{2+} , the CaCl_2 was reduced to 0.5 mM and the MgSO_4 was increased to 2 mM. Endplate recordings were performed as previously described (Wang et al., 2016; Wang and Rich, 2018). Briefly, the tibialis anterior muscle was pinned in a dish and stained with 10 μM 4-(4-diethylaminostyryl)-N-methylpyridinium iodide (Invitrogen) to visualize the NMJs. To eliminate contraction, 1–3 μM μ -conotoxin GIIIB (Peptide Institute) was applied to block muscle Na^+ channels. Muscle fibers were voltage-clamped at -70 mV . For all experiments, quantal content was calculated by dividing peak EPC amplitude by peak miniature EPC (mEPC) current amplitude. 3,4-DAP was applied at a dose of 100 μM .

Muscle force recordings were done at physiological temperature, whereas voltage-clamp recordings of NMJ function were performed at room temperature. As this difference in temperature could lead to different results, we confirmed the efficacy of 3,4-DAP in correcting NMJ transmission *in vivo*.

mRNA analyses

The lumbosacral spinal cord was removed from euthanized WT and $\text{BK}^{-/-}$ mice, frozen in liquid nitrogen, and stored at -80°C . Total RNA was isolated from spinal cord samples using the TRIzol technique. 1 μg RNA was reverse transcribed to synthesize cDNA with random primers. To quantify various *Kcna* (K_v1) and *Kcnc* (K_v3) channels and $\beta 2$ -microglobulin mRNA levels, real-time quantitative reverse transcription (RT)-PCR was performed with an MJ Research DNA engine Opticon 2 using Taqman gene-specific primers and probes (*Kcnal*, Mm00439977.s1; *Kcna2*, Mm00434584.s1; *Kcna4*, Mm00435241.s1; and $\beta 2$ -microglobulin, Mm00437762.m1) from Applied Biosystems (Thermo Fisher Scientific). Cycle thresholds were normalized to $\beta 2$ -microglobulin cycle thresholds and analyzed using the $\Delta\Delta\text{CT}$ method (Livak and Schmittgen, 2001).

Experimental design and statistical analysis

For voltage-clamp experiments, at least seven NMJs were recorded per muscle. For experiments in which drugs were given, the same muscle was studied before and after drug treatment. Nested analysis of variance (SYSTAT; Systat Software) was used for comparing the effect of drugs and other experimental manipulations. Averaged results are expressed as mean \pm SEM. P values < 0.05 and < 0.01 are denoted by one and two asterisks, respectively.

For force measurements, four WT and six $\text{BK}^{-/-}$ mice were used. For force experiments with 3,4-DAP, five WT and four

$\text{BK}^{-/-}$ mice were used. Force–frequency curves were generated and then fit with a Boltzmann sigmoidal curve. One-way ANOVA was performed to compare nerve versus muscle stimulation as well as with and without the drug. All error bars shown are \pm SEM.

Results

Muscle weakness in $\text{BK}^{-/-}$ mice was assessed in the plantar flexor (medial and lateral gastrocnemius, plantaris, and soleus) muscles by measuring *in vivo* muscle force via both sciatic nerve stimulation and direct muscle stimulation. To achieve direct muscle stimulation, α -BTX was injected into the muscle to block neuromuscular transmission and stimulating electrodes were placed above and below the plantar flexor muscles. An important consideration in assessing force production is muscle mass. The average weight of the plantar flexor muscles from the 2–4-mo-old $\text{BK}^{-/-}$ mice (0.14 ± 0.01 g) used in this study trended lower than in the age-matched WT mice (0.18 ± 0.01 g; $P = 0.088$). The potential impact of this on overall motor function depends on body weight. A previous study showed that $\text{BK}^{-/-}$ mice were smaller than WT littermates (Halm et al., 2017). In this study, the weight of $\text{BK}^{-/-}$ mice (19.7 ± 0.9 g) was also significantly lower than that of WT mice (24.6 ± 1.7 g; $P = 0.025$). The plantar flexor muscle weight to body weight ratio of $\text{BK}^{-/-}$ mice (0.0073 ± 0.0003) was not significantly different from WT (0.0073 ± 0.0001 ; $P = 0.975$), indicating that the reduction in $\text{BK}^{-/-}$ muscle weight was proportional to the reduction in body weight. To account for changes in muscle mass, we normalized the force to muscle weight (specific force).

Muscle force triggered by single action potentials (twitch), as well as by 30- and 60-Hz stimulation, is shown for $\text{BK}^{-/-}$ and WT muscle in response to stimulation of the sciatic nerve and direct muscle stimulation (Fig. 1 A). The peak twitch force of $\text{BK}^{-/-}$ muscle in response to nerve stimulation (4.00 ± 0.40 N/g) was significantly lower than in $\text{BK}^{-/-}$ muscle stimulated directly (7.60 ± 0.66 N/g; $P = 1.54 \times 10^{-4}$), WT muscle stimulated via nerve (6.82 ± 0.11 N/g; $P = 0.005$), or WT muscle stimulated directly (6.26 ± 0.21 N/g; $P = 0.023$; Fig. 1 B; one-way ANOVA, Tukey correction). The force–frequency relationship for WT muscle showed that nerve and direct muscle stimulation generated the same force at all frequencies (0.3–80 Hz; Fig. 1 C). In contrast, nerve-stimulated $\text{BK}^{-/-}$ muscle was weak at all frequencies compared with direct muscle stimulation. These data indicate that $\text{BK}^{-/-}$ muscle is significantly weak upon nerve stimulation but is capable of generating normal force at all frequencies with direct muscle stimulation. This strongly suggests that a defect in the motor axon or NMJ function is responsible for weakness in $\text{BK}^{-/-}$ mice.

To probe function of the NMJ, we performed voltage-clamp recordings of EPCs from the tibialis anterior muscle, as previously described (Wang et al., 2016). During these recordings, there was no failure of action potential invasion into the pre-synaptic terminal. These findings argue against a defect in function of the motor axon. EPC amplitude was reduced by >60% in $\text{BK}^{-/-}$ mice (Fig. 2 A). The reduction in EPC amplitude was not due to a change in the mEPC, as the mEPC amplitude was slightly

larger in $\text{BK}^{-/-}$ than WT mice (Fig. 2 B). The normal size of the mEPCs strongly suggests that postsynaptic acetylcholine receptors are expressed at normal levels in $\text{BK}^{-/-}$ mice. These data indicated that the number of vesicles released in response to a presynaptic action potential (quantal content) was reduced by close to 60%. This reduction was accompanied by a 70% reduction in the frequency of mEPCs in $\text{BK}^{-/-}$ muscle (1.1 ± 0.5 Hz) compared with WT (3.6 ± 0.3 Hz; Fig. 2).

Both the probability of vesicle release and the number of releasable vesicles contribute to quantal content (Bennett et al., 1975; Wang et al., 2010a, 2010b). We inferred the probability of release by examining short-term synaptic plasticity during repetitive stimulation. WT NMJs and other synapses with a high probability of release undergo depression (reduced release with repetitive stimulation), whereas NMJs and other synapses with a low probability of release undergo facilitation (increased release with repetitive stimulation; Zucker and Regehr, 2002; Wang et al., 2004). $\text{BK}^{-/-}$ NMJs underwent facilitation rather than depression during repetitive stimulation (Fig. 3). These data suggest that a reduction in the probability of release is an important contributor to the reduction in vesicle release in $\text{BK}^{-/-}$ NMJs.

The reduction in probability of vesicle release was a surprise, as loss of BK channels at the NMJ has generally been proposed to prolong the action potentials and increase Ca^{2+} entry (Robitaille and Charlton, 1992; Robitaille et al., 1993; Vatanpour and Harvey, 1995; Flink and Atchison, 2003; Ford and Davis, 2014; see, however, Pattillo et al., 2001). The reduction in the probability of release caused us to question whether the impact of lost BK channels was due to the loss of BK-mediated K^+ current. To investigate this, we applied three different BK channel blockers that have been used to probe channel function at the NMJ: 400 nM iberiotoxin, 10 μM paxilline, and 400 nM charybdotoxin (Robitaille and Charlton, 1992; Robitaille et al., 1993; Vatanpour and Harvey, 1995; Sugiura and Ko, 1997; Pattillo et al., 2001; Flink and Atchison, 2003). None of the toxins had a detectable effect on either quantal content or frequency of mEPCs (Table 1). Iberiotoxin and charybdotoxin were both purchased and tested from two vendors. These data suggest that K^+ current through BK channels has little to no effect on the function of the adult mouse NMJ.

Our results differ from previous studies of the mouse NMJ that suggested significantly increased release of vesicles following block of BK channels (Vatanpour and Harvey, 1995; Flink and Atchison, 2003). One previous study was performed using low extracellular Ca^{2+} to eliminate twitch (Vatanpour and Harvey, 1995). To determine whether this experimental difference could account for the difference in results, we tested the efficacy of BK channel blockers in a low Ca^{2+} /high Mg^{2+} solution similar to that used by Vatanpour and Harvey. None of the BK channel blockers tested increased quantal content in low- Ca^{2+} /high- Mg^{2+} solution (Table 2).

In *Drosophila melanogaster*, voltage-gated shaker (K_v) channels were shown to be up-regulated following knockout of BK channels, such that block of K_v channels with 4-aminopyridine caused a large increase in transmitter release at the NMJ (Lee et al., 2008; see, however, Warbington et al., 1996). This

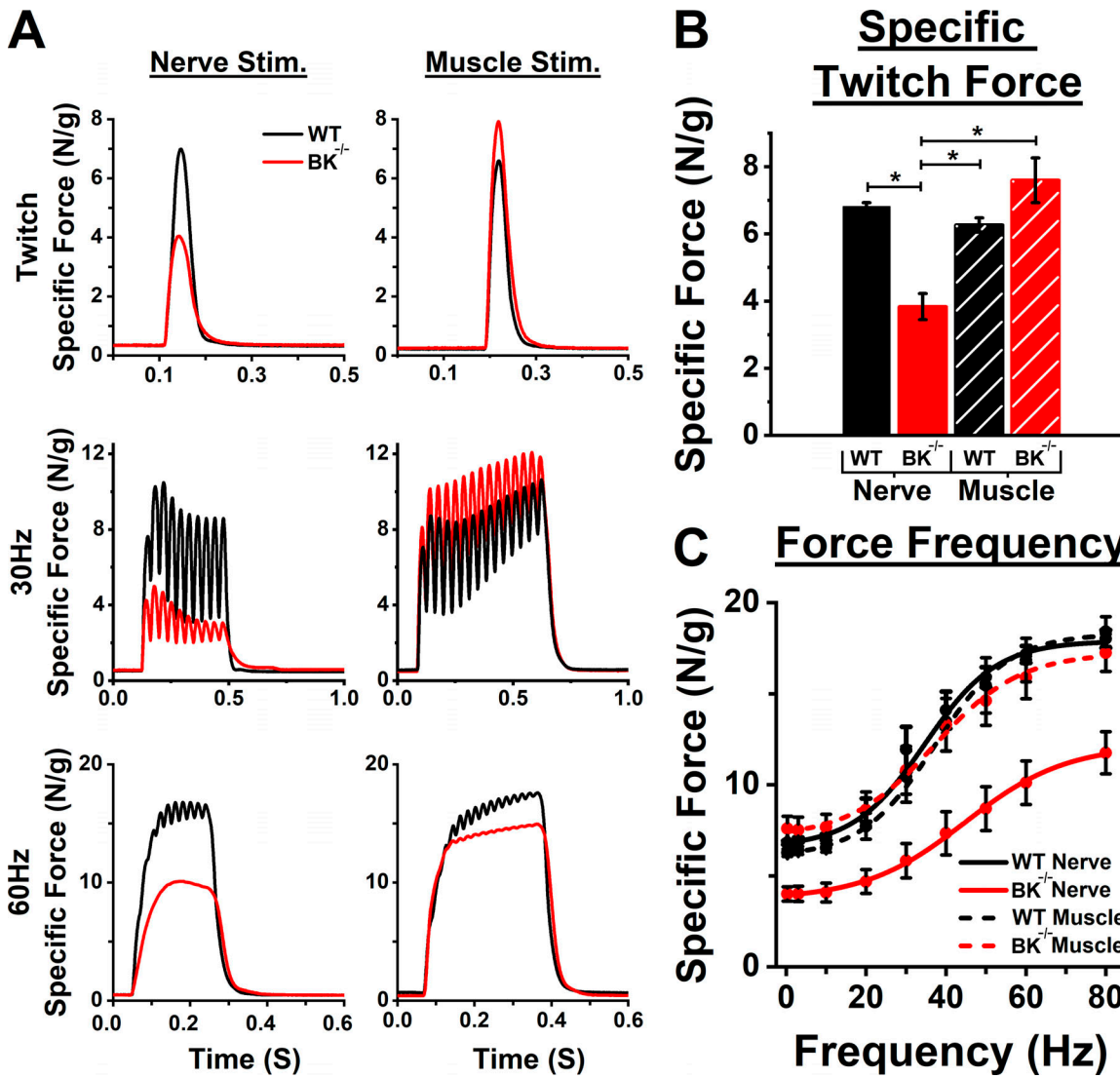


Figure 1. Weakness in $\text{BK}^{-/-}$ mice is due to neuromuscular dysfunction. (A) Representative specific force traces from WT (black) and $\text{BK}^{-/-}$ (red) muscle showing twitches (top panel) and responses to 30-Hz (middle panel) and 60-Hz (bottom panel) stimulation for both nerve stimulation (left column) and direct muscle stimulation (right column). (B) Bar graph showing twitch-specific force for nerve and muscle stimulation. Values shown as mean \pm SEM. *, $P < 0.05$, one-way ANOVA. (C) Specific force–frequency curves, fitted with a Boltzmann equation, for WT nerve (black solid line) and muscle (black dashed line) stimulation as well as $\text{BK}^{-/-}$ nerve (red solid line) and muscle (red dashed line) stimulation. Values are shown as \pm SEM. $n =$ four WT and six $\text{BK}^{-/-}$ mice.

treatment is thought to increase Ca^{2+} entry and vesicle release because the block of K_v channels widens the presynaptic action potential (Wang et al., 2016; Meriney et al., 2018; Ng et al., 2017). We tested the effect of the K_v channel blocker 3,4-DAP in WT and $\text{BK}^{-/-}$ NMJs (Fig. 4). Following the application of 3,4-DAP, the EPC amplitude and duration increased at both WT and $\text{BK}^{-/-}$ NMJs (Fig. 4 A). In WT NMJs, the increase in EPC amplitude was due to an increase in mEPC amplitude such that quantal content was minimally changed. While others have seen a similar increase in amplitude of miniature endplate potentials following treatment with 3,4-DAP (Mori et al., 2012; Ng et al., 2017), the mechanism underlying the increase has not been determined. If 3,4-DAP inhibits acetylcholinesterase, the increase in mEPC amplitude would be associated with a slowing of mEPC decay. Following addition of 3,4-DAP, the time constant of mEPC decay was significantly prolonged for WT from 1.05 ± 0.04 ms (five

mice, 42 NMJs) to 1.35 ± 0.04 ms (41 NMJs, $P < 0.01$) and for $\text{BK}^{-/-}$ from 0.93 ± 0.03 ms (42 NMJs) to 1.38 ± 0.03 ms (five mice, 49 NMJs, $P < 0.01$). These data support the possibility that 3,4-DAP has two effects on NMJ function that increase amplitude of the EPC: block of presynaptic K_v channels and partial block of acetylcholinesterase.

In $\text{BK}^{-/-}$ NMJs, a dramatic increase in EPC amplitude was due to both an increase in mEPC amplitude and a more than twofold increase of quantal content (Fig. 4 B). The block of K_v channels with 3,4-DAP also increased the frequency of spontaneous release, as has been reported by others (Ng et al., 2017). However, it did not eliminate the difference in frequency of spontaneous release of vesicles in WT versus $\text{BK}^{-/-}$ NMJs (Fig. 4). These data suggest that the defect in vesicle release at $\text{BK}^{-/-}$ NMJs cannot be fully explained by reduced voltage-dependent Ca^{2+} entry during action potentials. Nonetheless, the difference in quantal content

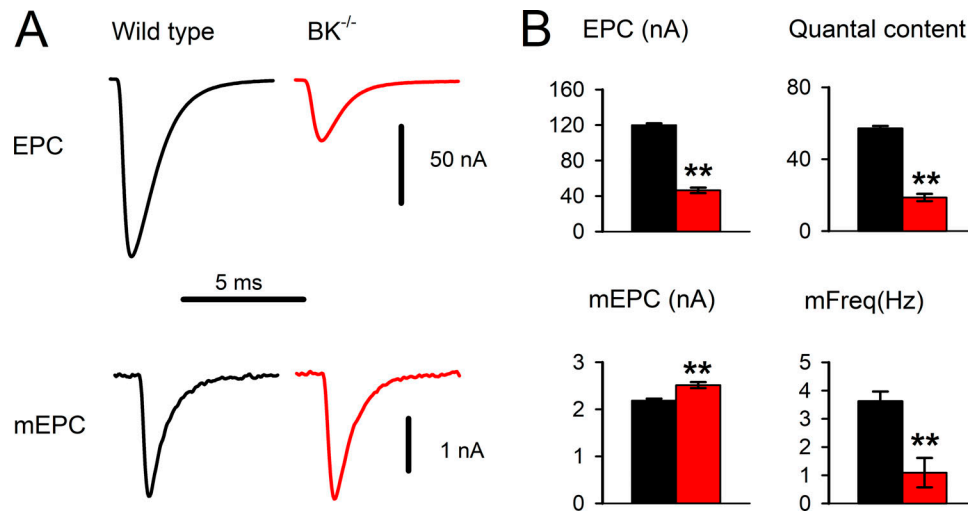


Figure 2. Vesicle release is reduced at the NMJ of $BK^{-/-}$ mice. (A) Representative average traces of the evoked EPC and the spontaneous mEPC from WT (black traces) and $BK^{-/-}$ (red traces) NMJs. **(B)** Plotted mean values for measures of synaptic function for WT (black) and $BK^{-/-}$ (red) NMJs. EPC and mEPC peak amplitudes were measured in nanoamps (nA); Quantal content is the number of vesicles released per presynaptic action potential (EPC peak amplitude/mEPC peak amplitude). mFreq, frequency of mEPCs in the absence of nerve stimulation. Values are shown as \pm SEM. **, $P < 0.01$. $n = 111$ NMJs from nine WT mice and 98 NMJs from eight $BK^{-/-}$ mice.

between WT and $BK^{-/-}$ NMJs could be eliminated by 3,4-DAP, which strongly suggests the number of releasable vesicles is normal, but the probability of release is reduced.

Given the similarity of our findings to those in *Drosophila*, we examined whether up-regulation of K_v channels occurred after elimination of BK channels. As an initial screen, we assayed levels of several K_v1 and K_v3 isoforms expressed by motor neurons (Brooke et al., 2004; Dufloq et al., 2011). The mRNA levels in the lumbosacral spinal cord of WT versus $BK^{-/-}$ mice were assessed by real-time quantitative RT-PCR relative to β -2-microglobulin mRNA for normalization purposes. There was no

up-regulation of the K_v1 and K_v3 isoforms measured in $BK^{-/-}$ mouse lumbosacral spinal cord (Table 3).

The normalization of evoked vesicle release in $BK^{-/-}$ NMJs by 3,4-DAP suggested administration of 3,4-DAP might normalize force production. To test this possibility, we performed nerve-stimulated force recordings with and without an intraperitoneal injection of 8 mg/kg 3,4-DAP (Fig. 5; Mori et al., 2012). After administration of 3,4-DAP, the force of the $BK^{-/-}$ nerve-stimulated twitch (Fig. 5 A) and tetanic contraction at 60 Hz (Fig. 5 B) dramatically increased. The peak twitch force of $BK^{-/-}$ muscle in the presence of 3,4-DAP (7.85 ± 0.51 N/g) was

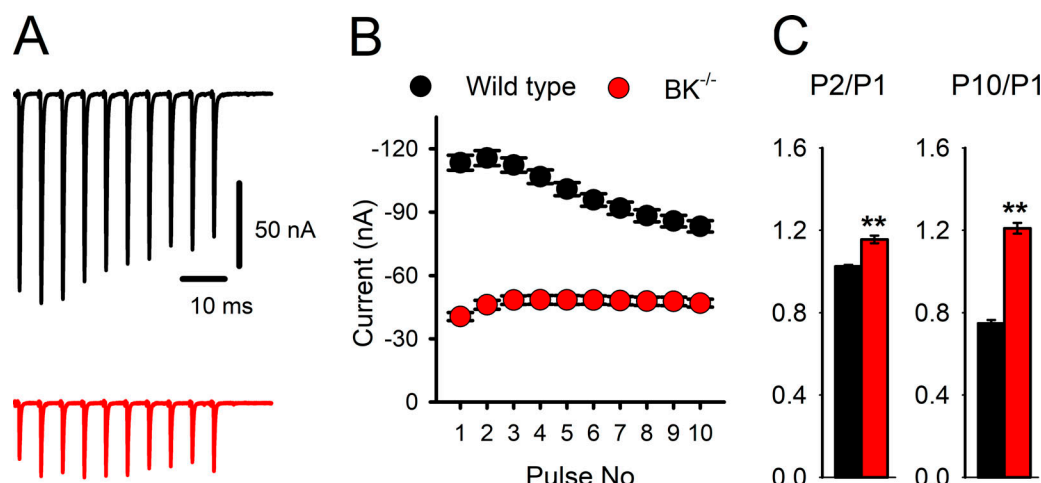


Figure 3. $BK^{-/-}$ NMJs exhibit facilitation rather than depression during repetitive stimulation. (A) 10 EPCs during a 50-Hz train of pulses for a representative WT (black) and $BK^{-/-}$ (red) NMJ. In both traces, stimulus artifacts were removed for clarity. **(B)** The change in average EPC amplitudes during the 50-Hz trains for WT and $BK^{-/-}$ NMJs. WT NMJs showed a slight increase in EPC amplitude early in the train of stimuli (facilitation); at the end of the train, EPC amplitude decreased below the initial value (depression). In $BK^{-/-}$ NMJs, facilitation was maintained throughout the train of stimuli. **(C)** Facilitation in $BK^{-/-}$ NMJs was significantly increased for both the second (P2/P1) and tenth stimuli (P10/P1) of the train (**, $P < 0.01$ versus WT for both comparisons). Values are shown as \pm SEM. $n = 93$ NMJs from nine WT mice and 83 NMJs from eight $BK^{-/-}$ mice.

Table 1. Effects of BK channel blockers on NMJ function in physiological solution

Toxin (company)	Number of mice (number of NMJs)	Results (before vs. after toxin)	Nested ANOVA (P value)
Iberiotoxin (Sigma-Aldrich), 400 nM	4 (43 before, 51 after)	Quantal content, 58.8 ± 2.6 vs. 60.0 ± 2.4; mFreq, 2.8 ± 0.7 vs. 4.0 ± 0.6	Quantal content, 0.825; mFreq, 0.224
Iberiotoxin (Cayman), 400 nM	3 (37 before, 50 after)	Quantal content, 41.5 ± 2.7 vs. 41.7 ± 2.2; mFreq, 3.58 ± 0.6 vs. 4.7 ± 0.5	Quantal content, 0.959; mFreq, 0.121
Charybdotoxin (Alomone), 400 nM	6 (70 before, 96 after)	Quantal content, 57.8 ± 1.8 vs. 55.3 ± 1.5; mFreq, 4.8 ± 0.7 vs. 4.8 ± 0.6	Quantal content, 0.287; mFreq, 0.926
Charybdotoxin (Cayman), 400 nM	3 (45 before, 56 after)	Quantal content, 57.9 ± 2.7 vs. 56.2 ± 2.4; mFreq, 6.1 ± 0.8 vs. 7.8 ± 0.7	Quantal content, 0.628; mFreq, 0.119
Paxilline (Sigma-Aldrich), 10 μM	5 (55 before, 63 after)	Quantal content, 48.6 ± 1.5 vs. 44.7 ± 1.7; mFreq, 4.6 ± 0.8 vs. 5.0 ± 0.9	Quantal content, 0.079; mFreq, 0.750

Results are shown as mean ± SEM. mFreq, frequency of mEPCs in the absence of nerve stimulation.

significantly higher than in the absence of 3,4-DAP (4.00 ± 0.40 N/g; $P = 0.003$), but not significantly different than WT in the presence (6.87 ± 0.99 N/g; $P = 0.709$) or absence (6.82 ± 0.11 ; $P = 0.712$) of 3,4-DAP (one-way ANOVA, Tukey correction). Similarly, at 60 Hz stimulation, the peak force of BK^{-/-} muscle in the presence of 3,4-DAP (19.12 ± 0.39 N/g) was significantly higher than in the absence of 3,4-DAP (10.11 ± 1.19 N/g; $P = 1.16 \times 10^{-4}$), but not significantly different than WT in the presence (14.95 ± 1.28 N/g; $P = 0.526$) or absence (16.86 ± 0.45 ; $P = 0.070$) of 3,4-DAP (one-way ANOVA, Tukey correction). As shown in Fig. 5 C, 3,4-DAP restored BK^{-/-} muscle force generation throughout the full force–frequency relationship (0.3–80 Hz).

Discussion

Nerve stimulation in BK^{-/-} mice led to significantly lower force production than in WT mice. However, force production via direct stimulation of muscle was normal, consistent with a defect in neuromuscular transmission. Voltage-clamp studies revealed reduced vesicle release at BK^{-/-} NMJs, which appeared to be due to a reduction in Ca²⁺ entry and subsequent decrease in the probability of vesicle release. The reduction in evoked vesicle release could be overcome by blocking K_v channels with 3,4-DAP to prolong nerve action potentials. Intraperitoneal injection of 3,4-DAP also normalized force production in vivo. Our study suggests that BK channels play a critical role in peripheral motor function such that mice lacking BK channels have reduced neuromuscular transmission that results in weakness.

Table 2. Effects of BK channel blockers on NMJ function in low-Ca²⁺ solution (0.5 mM Ca²⁺, 2 mM Mg²⁺)

Toxin (company)	Number of mice (number of NMJs)	Results (before vs. after toxin)	Nested ANOVA (P)
Iberiotoxin (Alomone), 400 nM	3 (47 before, 51 after)	Quantal content, 1.30 ± 0.09 vs. 1.35 ± 0.09; mFreq, 6.46 ± 1.68 vs. 8.39 ± 1.63	Quantal content, 0.705; mFreq, 0.412
Charybdotoxin (Alomone), 400 nM	3 (46 before, 50 after)	Quantal content, 1.50 ± 0.13 vs. 1.38 ± 0.12; mFreq, 3.69 ± 1.01 vs. 6.28 ± 0.99	Quantal content, 0.480; mFreq, 0.070
Paxilline (Sigma-Aldrich), 10 μM	3 (42 before, 43 after)	Quantal content, 0.92 ± 0.09 vs. 0.90 ± 0.08; mFreq, 6.41 ± 1.67 vs. 9.45 ± 1.61	Quantal content, 0.918; mFreq, 0.194

Results are shown as mean ± SEM. mFreq, frequency of mEPCs in the absence of nerve stimulation.

Weakness in BK^{-/-} mice is due to reduction of evoked acetylcholine release at the NMJ

BK^{-/-} mice exhibit significant motor dysfunction, including problems with balance and gait, as well as weak grip (Meredith et al., 2004; Sausbier et al., 2004; Chen et al., 2010; Typlt et al., 2013). These deficits highlight the importance of BK channels in the normal function of the motor system. However, given the widespread expression of BK channels in the nervous system, it is difficult to ascribe motor dysfunction to dysfunction of specific neurons. There is evidence that dysfunction of cerebellar circuits contributes to ataxia caused by knockout of BK channels (Sausbier et al., 2004; Chen et al., 2010). However, dysfunction of the cerebellum does not cause weakness; therefore, there must be dysfunction of other parts of the motor system. Because the reduction in force following nerve stimulation recorded here is close to the magnitude of reduction in grip strength previously reported in BK^{-/-} mice (Typlt et al., 2013), we posited that dysfunction of the NMJ is the primary contributor to weakness in BK^{-/-} mice.

Our findings raise the possibility that motor dysfunction in patients with BK channel mutations (Bailey et al., 2019) may be due in part to a presynaptic problem causing the failure of neuromuscular transmission. Lambert–Eaton myasthenic syndrome is another disorder where weakness is due to a reduction of presynaptic vesicle release (Elmqvist and Lambert, 1968; Engisch et al., 1999). Lambert–Eaton myasthenic syndrome responds well to treatment with 3,4-DAP to increase presynaptic Ca entry (Newsom-Davis, 2003; Sedehizadeh et al., 2012). As 3,4-DAP normalized force in BK null mice, it may be worth trying in patients with weakness in the setting of BK channel mutations.

The role of BK channels in function of the mouse NMJ

At the NMJ, it is proposed that Ca²⁺ current through Cav2.1 (P/Q) channels helps to activate BK channels, which shorten action potential duration to limit release (Robitaille and Charlton, 1992; Robitaille et al., 1993; Katz et al., 1997; Protti and Uchitel, 1997;

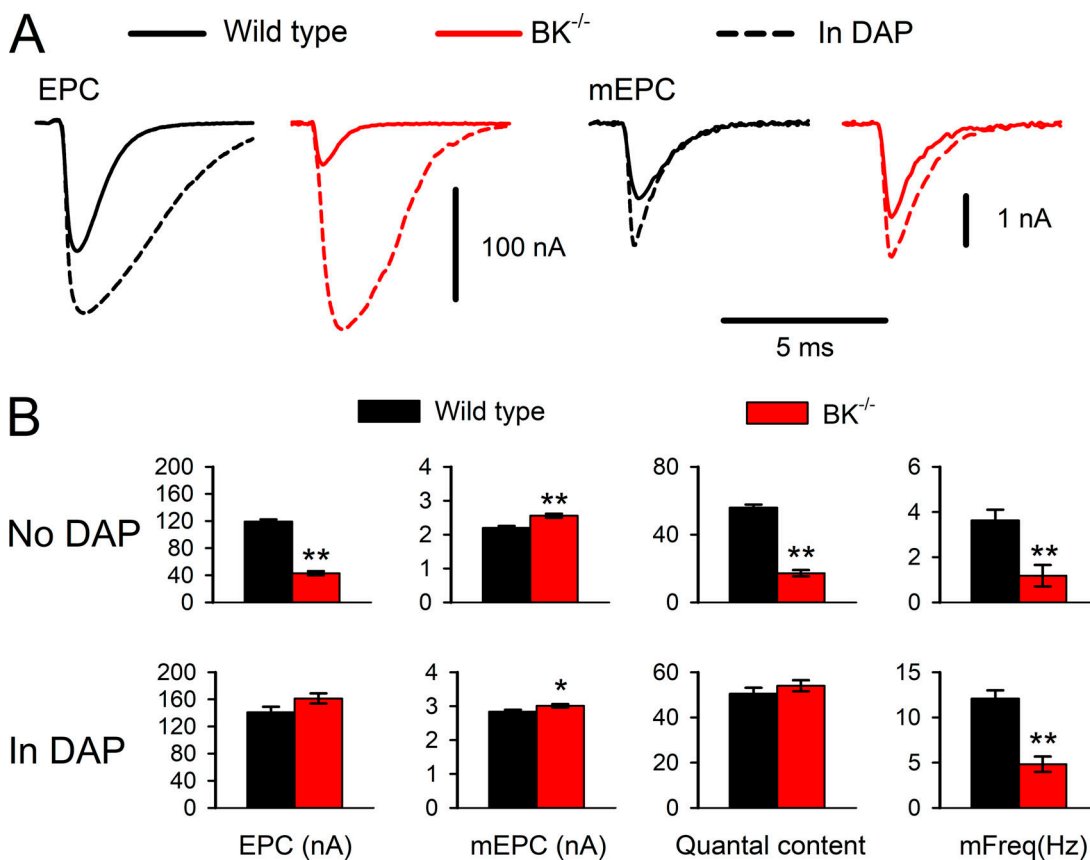


Figure 4. The reduction in vesicle release at $\text{BK}^{-/-}$ NMJs can be overcome by blocking voltage-gated K^+ channels. (A) Superimposed representative WT (black) and $\text{BK}^{-/-}$ (red) EPCs and mEPCs before (solid lines) and after (dashed lines) treatment with 100 μM 3,4-DAP. (B) Bar graphs show mean data \pm SEM. $n =$ five WT and five $\text{BK}^{-/-}$ mice. At least seven NMJs were recorded from each muscle. *, $P < 0.05$; **, $P < 0.01$.

Ford and Davis, 2014; Dittrich et al., 2018). One would thus expect block/loss of BK channels to increase release by widening the presynaptic action potential. In agreement with this expectation, increased release following block of BK channels has been reported at the mouse NMJ (Vatanpour and Harvey, 1995; Flink and Atchison, 2003).

Our results with blockers of BK channels differ from the previous studies of BK channel function at the mouse

NMJ. Varied results in the field include a study which found that the application of 300 nM charybdotoxin or 100 nM iberiotoxin caused a doubling of quantal content (Vatanpour and Harvey, 1995) and another which found that application of 150 nM iberiotoxin caused a doubling of the endplate potential (Flink and Atchison, 2003). There are some experimental differences between our studies and the previous studies, but none of them can easily explain the differing results. One study was performed using low extracellular Ca^{2+} to eliminate twitch (Vatanpour and Harvey, 1995), while the other crushed muscle fibers to eliminate twitch (Flink and Atchison, 2003). We found that blockers of BK channels had no effect on release when extracellular Ca^{2+} was decreased. Consequently, the discrepancy between results cannot be explained by differences in the level of extracellular Ca^{2+} .

We recorded using a preparation that is as close to physiological as possible, normal extracellular Ca^{2+} with intact muscle fibers, in which twitch was prevented with μ -conotoxin to block muscle Na^+ channels. Different studies also used different muscles. Moreover, the previous studies did not perform voltage clamp; as a result, their measures of changes in muscle membrane potential could be complicated by a change in muscle membrane properties after block of BK channels (Khedraki et al., 2017; Burke et al., 2018). Use of voltage clamp avoids this technical issue. We used three toxins, at higher doses than used previously, and found no change in evoked release. In some

Table 3. Spinal cord mRNA expression levels of *Kcna* (K_v1) and *Kcnc* (K_v3) isoforms

K channel isoform	WT	$\text{BK}^{-/-}$	t test
<i>Kcna1</i>	1.00 \pm 0.14	0.90 \pm 0.04	0.46
<i>Kcna2</i>	1.00 \pm 0.16	0.93 \pm 0.09	0.68
<i>Kcna4</i>	1.00 \pm 0.29	0.58 \pm 0.05	0.15
<i>Kcnc1</i>	1.00 \pm 0.19	1.27 \pm 0.25	0.38
<i>Kcnc2</i>	1.00 \pm 0.14	1.36 \pm 0.29	0.25
<i>Kcnc3</i>	1.00 \pm 0.10	1.05 \pm 0.17	0.79
<i>Kcnc4</i>	1.00 \pm 0.14	1.20 \pm 0.21	0.41

Real-time quantitative RT-PCR was performed on mRNA isolated from WT and $\text{BK}^{-/-}$ lumbosacral spinal cords. Expression levels were normalized to WT levels. All values are shown \pm SEM. $n =$ five spinal cords per group.

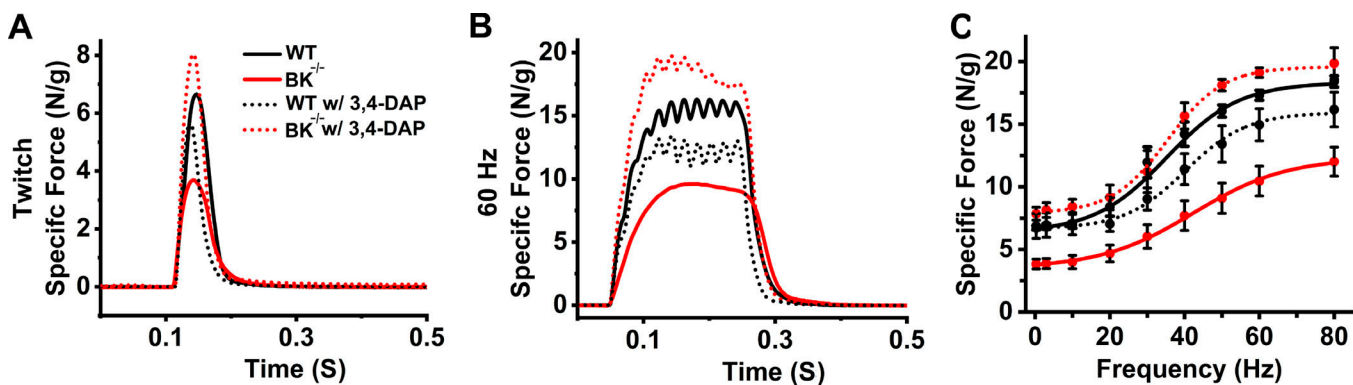


Figure 5. Normalization of $BK^{-/-}$ muscle force production following treatment with 3,4-DAP. (A and B) Representative twitch (A) and tetanic (60 Hz; B) muscle force traces following stimulation of the sciatic nerve of WT without (black solid line) and with 3,4-DAP (black dashed line) as well as $BK^{-/-}$ without (red solid line) and with 3,4-DAP (red dashed line). (C) Specific force–frequency curves, fitted with a Boltzmann equation. Values are mean \pm SEM. $n =$ five WT and four $BK^{-/-}$ mice.

cases, toxins were purchased from more than one supplier to minimize the possibility that lack of effect was due to the purchase of ineffective toxin. We conclude that K^+ current through BK channels has little to no effect on the function of the mature mouse NMJ in physiological conditions.

Despite the lack of effect of block of BK channels, knocking out BK channels had a dramatic effect on function of the NMJ. One possible explanation for this is that the defect in NMJ function in $BK^{-/-}$ mice arises from the method used to generate deletion of the channel. In the process of removing exon 1 to generate $BK^{-/-}$ mice, a neomycin-resistance cassette was retained in the $BK^{-/-}$ allele (Meredith et al., 2004). Retention of the PGK-neomycin (neomycin phosphotransferase gene with a phosphoglycerate kinase I promoter) can alter the expression of nearby genes (Olson et al., 1996; Pham et al., 1996; Scacheri et al., 2001). It is thus possible that the decreased release of acetylcholine reported here is a consequence of altered gene expression secondary to the retained neomycin gene. We do not favor this interpretation as two previous studies in *Drosophila*, which generated knockouts of the BK gene (slopoke) using different methods, found a similar reduction in neurotransmitter release at the NMJ (Warbington et al., 1996; Lee et al., 2008).

Another possibility is that there is a developmental effect leading to up-regulation of voltage-gated K^+ (K_v) channels, as has been reported following knockout of BK channels in *Drosophila* (Lee et al., 2008, 2014). Up-regulation of K_v channels might shorten the presynaptic action potential to reduce Ca^{2+} entry such that the probability of release is reduced (Dittrich et al., 2018). While we did not find evidence supporting up-regulation of K_v channels in the spinal cord, our study of K_v channels was not exhaustive, and it remains possible that other K_v channels not assayed are up-regulated. It is also possible that there is a developmental effect independent of up-regulation of K_v channels.

Another way in which knockout, but not block, of BK channels might reduce release is through modulation of presynaptic Ca^{2+} channels or the coupling of Ca^{2+} channels with synaptic vesicles. BK channels have been found to colocalize with presynaptic Ca^{2+} channels at the NMJ (Robitaille et al., 1993) and have recently been shown to modulate P/Q (Cav2.1) Ca^{2+} currents through direct

interaction (Dolphin, 2018; Zhang et al., 2018). P/Q-type Ca^{2+} channels play a central role in triggering vesicle release at the mouse NMJ (Uchitel et al., 1992; Hong and Chang, 1995; Wang et al., 2004). The modulation could occur via changes in either the number of channels present or the functional properties of the channels.

Our data are the first we are aware of to directly demonstrate that a defect in synaptic transmission in $BK^{-/-}$ mice does not arise from absence of BK current per se at the synapse. Instead, our data suggest that the BK channel plays a central role in development of the NMJ via modulation of presynaptic Ca^{2+} current or the effectiveness of Ca^{2+} in triggering release. In the absence of functional BK channels, vesicle release is reduced enough *in vivo* to cause failure of neuromuscular transmission and weakness.

Acknowledgments

Christopher J. Lingle served as editor.

We thank Dan Halm for helpful discussions and Andrea Meredith for providing the initial breeding pairs of $BK^{-/-}$ mice.

This work was supported by National Institutes of Health grant AR074985 (M.M. Rich) and National Institute of Neurological Disorders and Stroke grant R15NS099850 (A.A. Voss).

The authors declare no competing financial interests.

Author contributions: X. Wang, S.R.A. Burke, and R.J. Talmadge performed experiments, analyzed and interpreted data, and helped write the manuscript. A.A. Voss and M.M. Rich designed experiments and wrote the manuscript.

Submitted: 3 November 2019

Revised: 27 January 2020

Accepted: 2 March 2020

References

- Bailey, C.S., H.J. Moldenhauer, S.M. Park, S. Keros, and A.L. Meredith. 2019. KCNMA1-linked channelopathy. *J. Gen. Physiol.* 151:1173–1189. <https://doi.org/10.1085/jgp.201912457>
- Bennett, M.R., T. Florin, and R. Hall. 1975. The effect of calcium ions on the binomial statistic parameters which control acetylcholine release at

synapses in striated muscle. *J. Physiol.* 247:429–446. <https://doi.org/10.1113/jphysiol.1975.sp010939>

Berkefeld, H., B. Fakler, and U. Schulte. 2010. Ca₂₊-activated K⁺ channels: from protein complexes to function. *Physiol. Rev.* 90:1437–1459. <https://doi.org/10.1152/physrev.00049.2009>

Brooke, R.E., T.S. Moores, N.P. Morris, S.H. Parson, and J. Deuchars. 2004. Kv3 voltage-gated potassium channels regulate neurotransmitter release from mouse motor nerve terminals. *Eur. J. Neurosci.* 20:3313–3321. <https://doi.org/10.1111/j.1460-9568.2004.03730.x>

Burke, S.R.A., E.J. Reed, S.H. Romer, and A.A. Voss. 2018. Levator Auris Longus Preparation for Examination of Mammalian Neuromuscular Transmission Under Voltage Clamp Conditions. *J. Vis. Exp.* (135). <https://doi.org/10.3791/57482>

Chen, X., Y. Kovalchuk, H. Adelsberger, H.A. Henning, M. Sausbier, G. Wietzorek, P. Ruth, Y. Yarom, and A. Konnerth. 2010. Disruption of the olivo-cerebellar circuit by Purkinje neuron-specific ablation of BK channels. *Proc. Natl. Acad. Sci. USA.* 107:12323–12328. <https://doi.org/10.1073/pnas.1001745107>

Dinardo, M.M., G. Camerino, A. Mele, R. Latorre, D. Conte Camerino, and D. Tricarico. 2012. Splicing of the rSlo gene affects the molecular composition and drug response of Ca₂₊-activated K⁺ channels in skeletal muscle. *PLoS One.* 7:e40235. <https://doi.org/10.1371/journal.pone.0040235>

Dittrich, M., A.E. Homan, and S.D. Meriney. 2018. Presynaptic mechanisms controlling calcium-triggered transmitter release at the neuromuscular junction. *Curr. Opin. Physiol.* 4:15–24. <https://doi.org/10.1016/j.cophys.2018.03.004>

Dolphin, A.C. 2018. Voltage-gated calcium channel $\alpha_2\delta$ subunits: an assessment of proposed novel roles. *F1000 Res.* 7:F1000 Faculty Rev-1830. <https://doi.org/10.12688/f1000research.16104.1>

Duflocoq, A., F. Chareyre, M. Giovannini, F. Couraud, and M. Davenne. 2011. Characterization of the axon initial segment (AIS) of motor neurons and identification of a para-AIS and a juxtapara-AIS, organized by protein 4.1B. *BMC Biol.* 9:66. <https://doi.org/10.1186/1741-7007-9-66>

Dupont, C., K.S. Denman, A.A. Hawash, A.A. Voss, and M.M. Rich. 2019. Treatment of myotonia congenita with retigabine in mice. *Exp. Neurol.* 315:52–59. <https://doi.org/10.1016/j.expneurol.2019.02.002>

Elmqvist, D., and E.H. Lambert. 1968. Detailed analysis of neuromuscular transmission in a patient with the myasthenic syndrome sometimes associated with bronchogenic carcinoma. *Mayo Clin. Proc.* 43:689–713.

Engisch, K.L., M.M. Rich, N. Cook, and M.C. Nowycky. 1999. Lambert-Eaton antibodies inhibit Ca₂₊ currents but paradoxically increase exocytosis during stimulus trains in bovine adrenal chromaffin cells. *J. Neurosci.* 19: 3384–3395. <https://doi.org/10.1523/JNEUROSCI.19-09-03384.1999>

Flink, M.T., and W.D. Atchison. 2003. Iberiotoxin-induced block of Ca₂₊-activated K⁺ channels induces dihydropyridine sensitivity of ACh release from mammalian motor nerve terminals. *J. Pharmacol. Exp. Ther.* 305:646–652. <https://doi.org/10.1124/jpet.102.046102>

Ford, K.J., and G.W. Davis. 2014. Archaerhodopsin voltage imaging: synaptic calcium and BK channels stabilize action potential repolarization at the *Drosophila* neuromuscular junction. *J. Neurosci.* 34:14517–14525. <https://doi.org/10.1523/JNEUROSCI.2203-14.2014>

Halm, S.T., M.A. Bottomley, M.M. Almutairi, M. Di Fulvio, and D.R. Halm. 2017. Survival and growth of C57BL/6J mice lacking the BK channel, *Kcnma1*: lower adult body weight occurs together with higher body fat. *Physiol. Rep.* 5:e13137. <https://doi.org/10.14814/phy2.13137>

Hong, S.J., and C.C. Chang. 1995. Inhibition of acetylcholine release from mouse motor nerve by a P-type calcium channel blocker, omega-agatoxin IVA. *J. Physiol.* 482:283–290. <https://doi.org/10.1113/jphysiol.1995.sp020517>

Katz, E., D.A. Protti, P.A. Ferro, M.D. Rosato Siri, and O.D. Uchitel. 1997. Effects of Ca₂₊ channel blocker neurotoxins on transmitter release and presynaptic currents at the mouse neuromuscular junction. *Br. J. Pharmacol.* 121:1531–1540. <https://doi.org/10.1038/sj.bjp.0701290>

Khedraki, A., E.J. Reed, S.H. Romer, Q. Wang, W. Romine, M.M. Rich, R.J. Talmadge, and A.A. Voss. 2017. Depressed Synaptic Transmission and Reduced Vesicle Release Sites in Huntington's Disease Neuromuscular Junctions. *J. Neurosci.* 37:8077–8091. <https://doi.org/10.1523/JNEUROSCI.0313-17.2017>

Lee, J., A. Ueda, and C.F. Wu. 2008. Pre- and post-synaptic mechanisms of synaptic strength homeostasis revealed by slowpoke and shaker K⁺ channel mutations in *Drosophila*. *Neuroscience*. 154:1283–1296. <https://doi.org/10.1016/j.neuroscience.2008.04.043>

Lee, J., A. Ueda, and C.F. Wu. 2014. Distinct roles of *Drosophila* cacophony and Dmca1D Ca(2+) channels in synaptic homeostasis: genetic interactions with slowpoke Ca(2+) -activated BK channels in presynaptic excitability and postsynaptic response. *Dev. Neurobiol.* 74:1–15. <https://doi.org/10.1002/dneu.22120>

Livak, K.J., and T.D. Schmittgen. 2001. Analysis of relative gene expression data using real-time quantitative PCR and the 2(-Delta Delta C(T)) Method. *Methods.* 25:402–408. <https://doi.org/10.1006/meth.2001.1262>

Meredith, A.L., K.S. Thorneloe, M.E. Werner, M.T. Nelson, and R.W. Aldrich. 2004. Overactive bladder and incontinence in the absence of the BK large conductance Ca₂₊-activated K⁺ channel. *J. Biol. Chem.* 279: 36746–36752. <https://doi.org/10.1074/jbc.M405621200>

Meriney, S.D., T.B. Tarr, K.S. Ojala, M. Wu, Y. Li, D. Lacomis, A. Garcia-Ocaña, M. Liang, G. Valdomir, and P. Wipf. 2018. Lambert-Eaton myasthenic syndrome: mouse passive-transfer model illuminates disease pathology and facilitates testing therapeutic leads. *Ann. N. Y. Acad. Sci.* 1412:73–81. <https://doi.org/10.1111/nyas.13512>

Mori, S., M. Kishi, S. Kubo, T. Akiyoshi, S. Yamada, T. Miyazaki, T. Konishi, N. Maruyama, and K. Shigemoto. 2012. 3,4-Diaminopyridine improves neuromuscular transmission in a MuSK antibody-induced mouse model of myasthenia gravis. *J. Neuroimmunol.* 245:75–78. <https://doi.org/10.1016/j.jneuroim.2012.02.010>

Newsom-Davis, J. 2003. Therapy in myasthenia gravis and Lambert-Eaton myasthenic syndrome. *Semin. Neurol.* 23:191–198. <https://doi.org/10.1055/s-2003-41135>

Ng, F., D.C. Lee, L.A. Schrumpf, M.E. Mazurek, V. Lee Lo, S.K. Gill, and R.A. Maselli. 2017. Effect of 3,4-diaminopyridine at the murine neuromuscular junction. *Muscle Nerve*. 55:223–231. <https://doi.org/10.1002/mus.25208>

Olson, E.N., H.H. Arnold, P.W. Rigby, and B.J. Wold. 1996. Know your neighbors: three phenotypes in null mutants of the myogenic bHLH gene MRF4. *Cell.* 85:1–4. [https://doi.org/10.1016/S0092-8674\(00\)81073-9](https://doi.org/10.1016/S0092-8674(00)81073-9)

Pattillo, J.M., B. Yazejian, D.A. DiGregorio, J.L. Vergara, A.D. Grinnell, and S.D. Meriney. 2001. Contribution of presynaptic calcium-activated potassium currents to transmitter release regulation in cultured *Xenopus* nerve-muscle synapses. *Neuroscience*. 102:229–240. [https://doi.org/10.1016/S0306-4522\(00\)00453-X](https://doi.org/10.1016/S0306-4522(00)00453-X)

Pham, C.T., D.M. MacIvor, B.A. Hug, J.W. Heusel, and T.J. Ley. 1996. Long-range disruption of gene expression by a selectable marker cassette. *Proc. Natl. Acad. Sci. USA.* 93:13090–13095. <https://doi.org/10.1073/pnas.93.23.13090>

Protti, D.A., and O.D. Uchitel. 1997. P/Q-type calcium channels activate neighboring calcium-dependent potassium channels in mouse motor nerve terminals. *Pflugers Arch.* 434:406–412. <https://doi.org/10.1007/s004240050414>

Robitaille, R., and M.P. Charlton. 1992. Presynaptic calcium signals and transmitter release are modulated by calcium-activated potassium channels. *J. Neurosci.* 12:297–305. <https://doi.org/10.1523/JNEUROSCI.12-01-00297.1992>

Robitaille, R., M.L. Garcia, G.J. Kaczorowski, and M.P. Charlton. 1993. Functional colocalization of calcium and calcium-gated potassium channels in control of transmitter release. *Neuron.* 11:645–655. [https://doi.org/10.1016/0896-6273\(93\)90076-4](https://doi.org/10.1016/0896-6273(93)90076-4)

Rüttiger, L., M. Sausbier, U. Zimmermann, H. Winter, C. Braig, J. Engel, M. Knirsch, C. Arntz, P. Langer, B. Hirt, et al. 2004. Deletion of the Ca₂₊-activated potassium (BK) alpha-subunit but not the BKbeta1-subunit leads to progressive hearing loss. *Proc. Natl. Acad. Sci. USA.* 101: 12922–12927. <https://doi.org/10.1073/pnas.0402660101>

Salkoff, L., A. Butler, G. Ferreira, C. Santi, and A. Wei. 2006. High-conductance potassium channels of the SLO family. *Nat. Rev. Neurosci.* 7:921–931. <https://doi.org/10.1038/nrn1992>

Sausbier, M., H. Hu, C. Arntz, S. Feil, S. Kamm, H. Adelsberger, U. Sausbier, C.A. Sailer, R. Feil, F. Hofmann, et al. 2004. Cerebellar ataxia and Purkinje cell dysfunction caused by Ca₂₊-activated K⁺ channel deficiency. *Proc. Natl. Acad. Sci. USA.* 101:9474–9478. <https://doi.org/10.1073/pnas.0401702101>

Sausbier, M., C. Arntz, I. Bucurenciu, H. Zhao, X.B. Zhou, U. Sausbier, S. Feil, S. Kamm, K. Essin, C.A. Sailer, et al. 2005. Elevated blood pressure linked to primary hyperaldosteronism and impaired vasodilation in BK channel-deficient mice. *Circulation.* 112:60–68. <https://doi.org/10.1161/01.CIR.0000156448.74296.FE>

Scacheri, P.C., J.S. Crabtree, E.A. Novotny, L. Garrett-Beal, A. Chen, K.A. Edgemon, S.J. Marx, A.M. Spiegel, S.C. Chandrasekharappa, and F.S. Collins. 2001. Bidirectional transcriptional activity of PGK-neomycin and unexpected embryonic lethality in heterozygote chimeric knockout mice. *Genesis.* 30:259–263. <https://doi.org/10.1002/geno.1027>

Sedehizadeh, S., M. Keogh, and P. Maddison. 2012. The use of aminopyridines in neurological disorders. *Clin. Neuropharmacol.* 35:191–200. <https://doi.org/10.1097/WNF.0b013e31825a68c5>

Sugiura, Y., and C.P. Ko. 1997. Novel modulatory effect of L-type calcium channels at newly formed neuromuscular junctions. *J. Neurosci.* 17: 1101–1111. <https://doi.org/10.1523/JNEUROSCI.17-03-01101.1997>

Tricarico, D., M. Barbieri, A. Mele, G. Carbonara, and D.C. Camerino. 2004. Carbonic anhydrase inhibitors are specific openers of skeletal muscle BK channel of K⁺-deficient rats. *FASEB J.* 18:760–761. <https://doi.org/10.1096/fj.03-0722fje>

Typlt, M., M. Mirkowski, E. Azzopardi, L. Ruettiger, P. Ruth, and S. Schmid. 2013. Mice with deficient BK channel function show impaired prepulse inhibition and spatial learning, but normal working and spatial reference memory. *PLoS One.* 8:e81270. <https://doi.org/10.1371/journal.pone.0081270>

Uchitel, O.D., D.A. Protti, V. Sanchez, B.D. Cherksey, M. Sugimori, and R. Llinás. 1992. P-type voltage-dependent calcium channel mediates presynaptic calcium influx and transmitter release in mammalian synapses. *Proc. Natl. Acad. Sci. USA.* 89:3330–3333. <https://doi.org/10.1073/pnas.89.8.3330>

Vatanpour, H., and A.L. Harvey. 1995. Modulation of acetylcholine release at mouse neuromuscular junctions by interaction of three homologous scorpion toxins with K⁺ channels. *Br. J. Pharmacol.* 114:1502–1506. <https://doi.org/10.1111/j.1476-5381.1995.tb13377.x>

Wang, X., and M.M. Rich. 2018. Homeostatic synaptic plasticity at the neuromuscular junction in myasthenia gravis. *Ann. N. Y. Acad. Sci.* 1412: 170–177. <https://doi.org/10.1111/nyas.13472>

Wang, X., K.L. Engisch, Y. Li, M.J. Pinter, T.C. Cope, and M.M. Rich. 2004. Decreased synaptic activity shifts the calcium dependence of release at the mammalian neuromuscular junction in vivo. *J. Neurosci.* 24: 10687–10692. <https://doi.org/10.1523/JNEUROSCI.2755-04.2004>

Wang, X., M.J. Pinter, and M.M. Rich. 2010a. Ca²⁺ dependence of the binomial parameters p and n at the mouse neuromuscular junction. *J. Neurophysiol.* 103:659–666. <https://doi.org/10.1152/jn.00708.2009>

Wang, X., Q. Wang, K.L. Engisch, and M.M. Rich. 2010b. Activity-dependent regulation of the binomial parameters p and n at the mouse neuromuscular junction in vivo. *J. Neurophysiol.* 104:2352–2358. <https://doi.org/10.1152/jn.00460.2010>

Wang, B., D.B. Jaffe, and R. Brenner. 2014. Current understanding of iberiotoxin-resistant BK channels in the nervous system. *Front. Physiol.* 5:382. <https://doi.org/10.3389/fphys.2014.00382>

Wang, X., M.J. Pinter, and M.M. Rich. 2016. Reversible Recruitment of a Homeostatic Reserve Pool of Synaptic Vesicles Underlies Rapid Homeostatic Plasticity of Quantal Content. *J. Neurosci.* 36:828–836. <https://doi.org/10.1523/JNEUROSCI.3786-15.2016>

Warbington, L., T. Hillman, C. Adams, and M. Stern. 1996. Reduced transmitter release conferred by mutations in the slowpoke-encoded Ca²⁺-activated K⁺ channel gene of *Drosophila*. *Invert. Neurosci.* 2:51–60. <https://doi.org/10.1007/BF02336660>

Zhang, F.X., V.M. Gadotti, I.A. Souza, L. Chen, and G.W. Zamponi. 2018. BK Potassium Channels Suppress Cav α 2δ Subunit Function to Reduce Inflammatory and Neuropathic Pain. *Cell Rep.* 22:1956–1964. <https://doi.org/10.1016/j.celrep.2018.01.073>

Zucker, R.S., and W.G. Regehr. 2002. Short-term synaptic plasticity. *Annu. Rev. Physiol.* 64:355–405. <https://doi.org/10.1146/annurev.physiol.64.092501.114547>